

SUPPLEMENTARY FIGURES

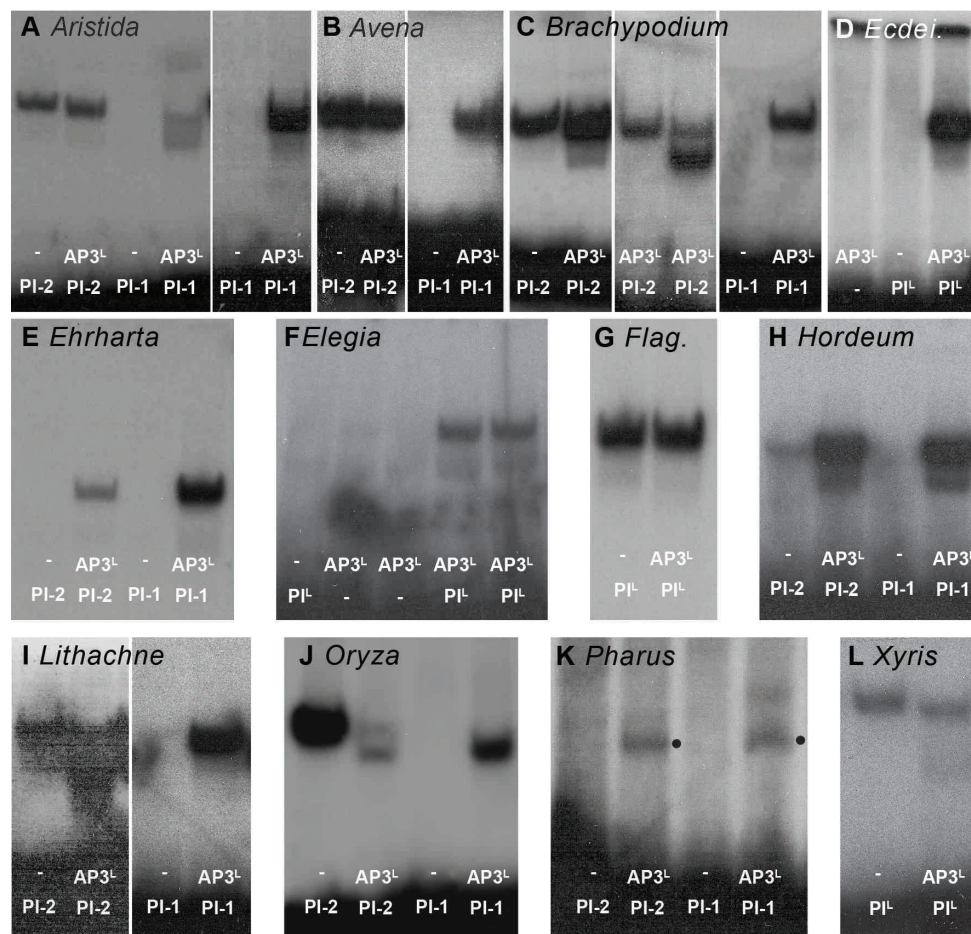


Figure S1. Gel shift assays for B-class proteins from taxa spanning the Poales. (A) *Aristida purpurea* PI-2 can form homodimers, PI-1 forms obligate heterodimers with AP3^L proteins. AP3^L protein in the first panel is SI1. AP3^L protein in the second panel is *Pharus virescens* AP3 (B) *Avena strigosa* PI-2 can form homodimers, PI-1 forms obligate heterodimers with AP3^L proteins. AP3^L protein in the left panel is J-AP3-C. AP3^L protein in the right panel is SI1-C. (C) *Brachypodium distachyon* PI-2 (BdSTS1) can form homodimers (left panel) and heterodimers with AP3^L proteins (middle panel). *B. distachyon* PI-1 forms obligate heterodimers with AP3^L proteins (right panel). AP3^L protein in the left and right panels is *B. distachyon* AP3. AP3^L protein in the middle panel is SI1-C. (D) *Ecdeiocolea monostachya* PI forms obligate heterodimers with its cognate AP3. (E) *Ehrharta erecta* PI-1 and PI-2 both form obligate heterodimers with J-AP3. (F) Both AP3^L proteins and the single PI^L protein from *Elegia elephas* form obligate heterodimers. (G) The PI^L protein from *Flagellaria indica* can form homodimers. AP3^L protein in lane 2 is J-AP3. (H) *Hordeum vulgare* PI-2 can form homodimers, PI-1 forms obligate heterodimers with AP3^L proteins. AP3^L protein in lanes 2 and 4 is from *Hordeum vulgare*. (I) *Lithachne humilis* PI-2 can form homodimers, PI-1 forms obligate heterodimers with AP3^L proteins. AP3^L protein in the first panel is SI-C. AP3^L protein in the second panel is J-AP3-C. (J) *Oryza sativa* PI-2 can form homodimers, PI-1 forms obligate heterodimers with AP3^L proteins. AP3^L protein in lanes 2 and 4 is SI1-C. (K) Neither PI-2 nor PI-1 from *Pharus virescens* reliably formed homodimers or obligate heterodimers with AP3^L proteins. AP3^L protein in lanes 2 and 4 is SI1-C. •= SI1-C homodimer band. (L) *Xyris lanata* PI can form homodimers. AP3^L protein in lane 2 is SI1-C.

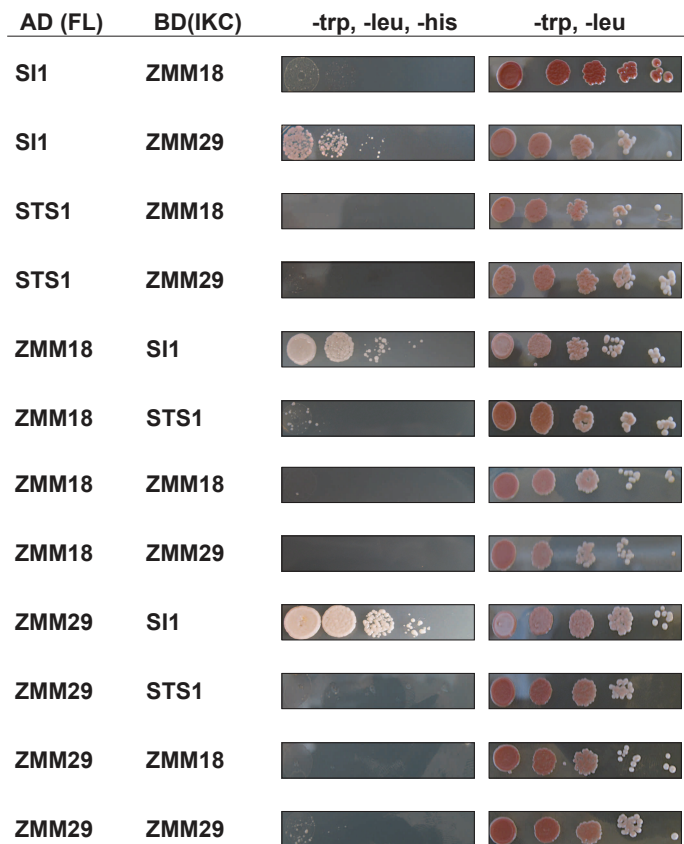


Figure S2. ZMM18, ZMM29 form obligate heterodimers with SI1 in yeast two-hybrid assays. Full-length B-class coding sequences were tested for their interactions with IKC constructs (missing the MADS-box domain).

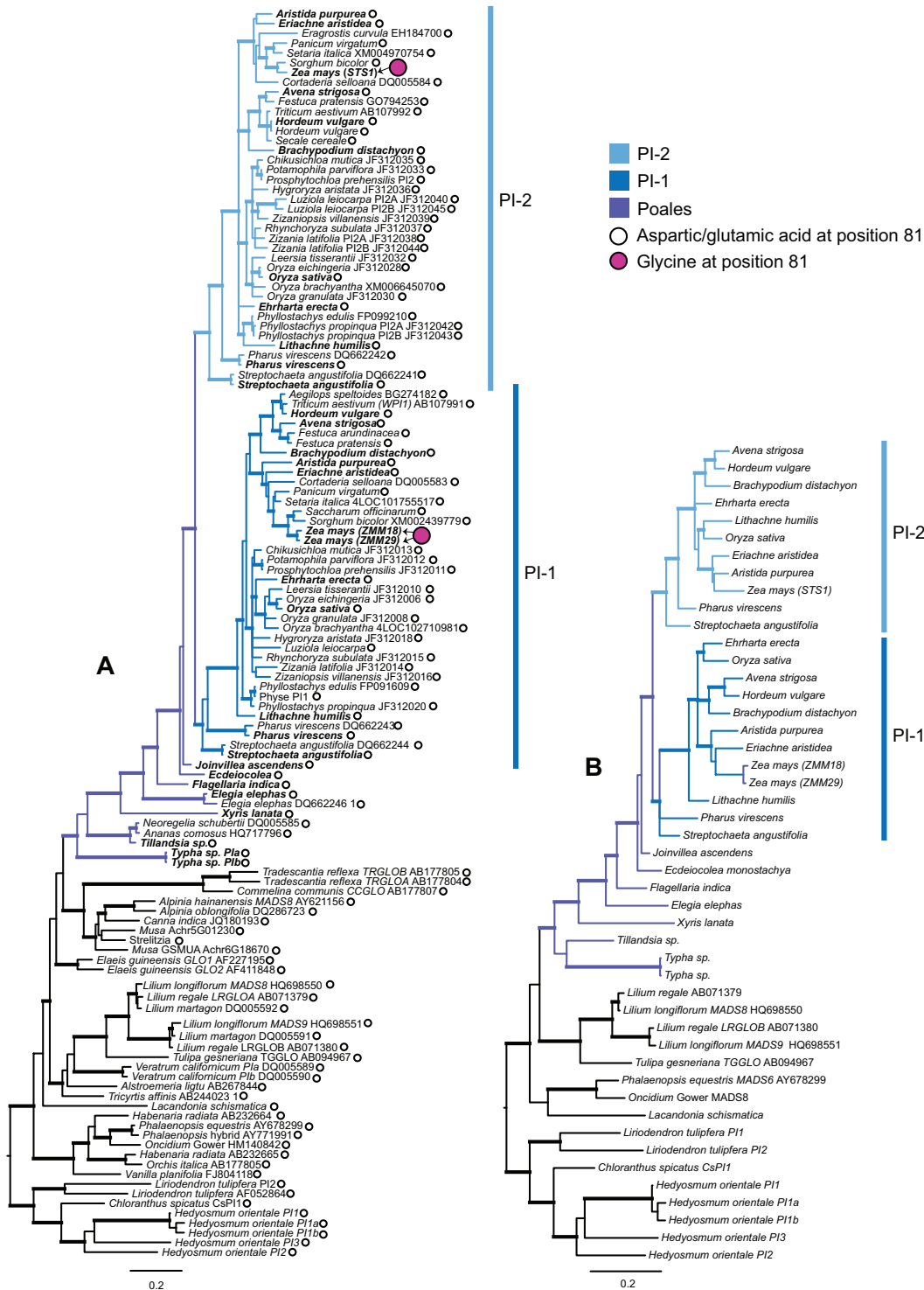


Figure S3. Bayesian phylogenetic analysis of PI^L gene sequences. (A) Full analysis, including a larger set of grass sequences retrieved from Genbank. (B) Analysis of only those sequences assessed for their ability to form homo- and heterodimers. Thickened branches indicate posterior probability > 0.95 . A glycine at position 81 of the PI^L amino acid alignment occurs only in the three PI^L proteins of *Zea mays* in our datasets.

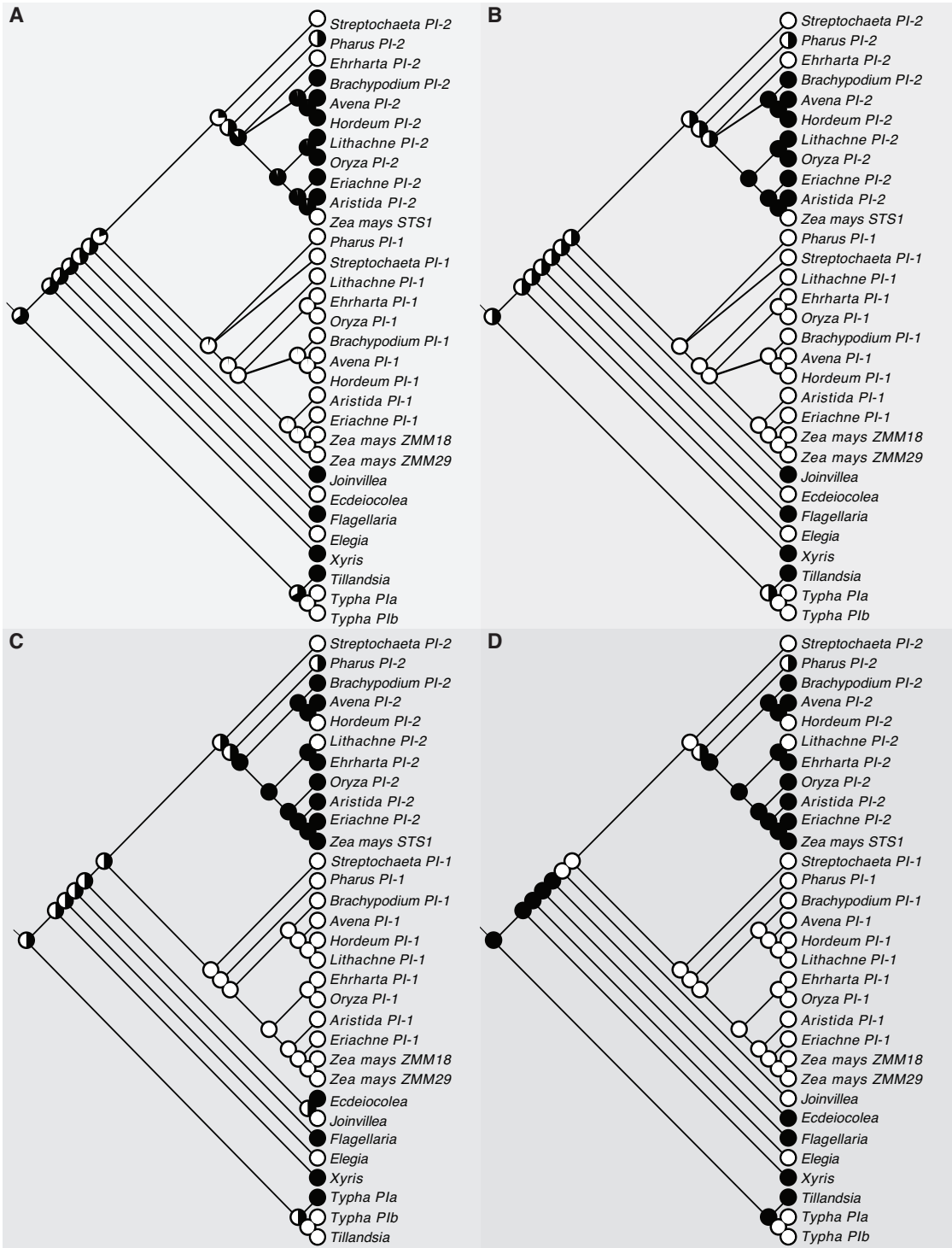


Figure S4. Reconstructions of ancestral dimerization state, depending on tree topology and outgroup selection. Likelihood (A) and parsimony (B) ancestral state reconstructions with all non-Poalean outgroups removed. (C) Parsimony ancestral reconstruction states with relationships within drawn according to (GPWG II 2012) (grasses) and (Bouchenak-Khelladi, et al. 2014) (broader Poales). (D) Parsimony ancestral reconstruction states with relationships within drawn according to (GPWG II 2012) (grasses) and (Givnish, et al. 2010) (broader Poales).

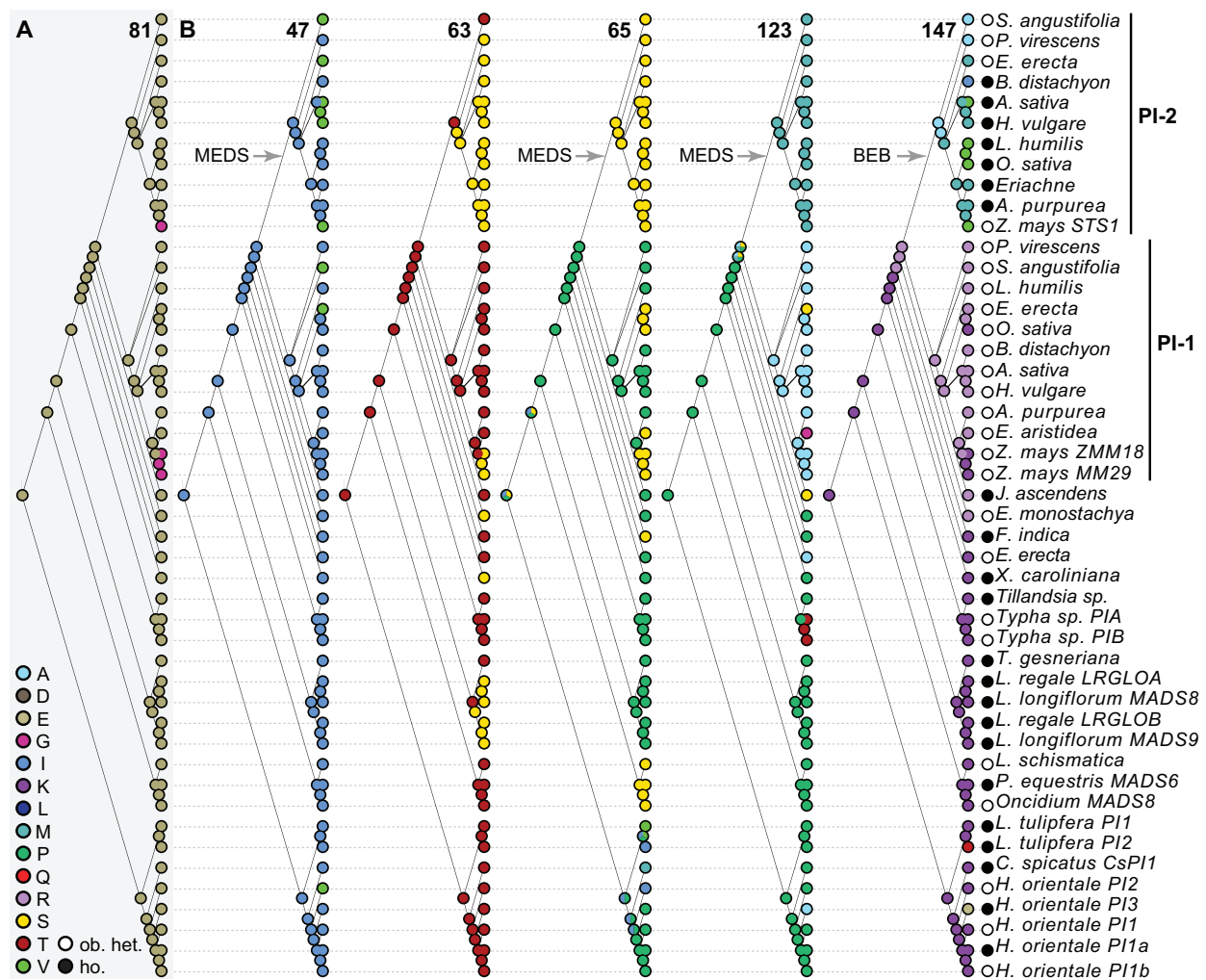


Figure S5. Key PI^{L} amino acid residues. (A) Gly81 is particular to PI^{L} proteins from *Zea mays*. All other PI^{L} proteins in our analyses have a glutamate at position 81. (B) Patterns of amino acid change across the PI^{L} phylogeny at select sites predicted to be evolving under positive selection. Dimerization state indicated next to gene names. Black= PI^{L} homodimerization, white = obligate heterodimerization. Arrows indicate the tested foreground lineage selected in the BEB and MEDS analyses.

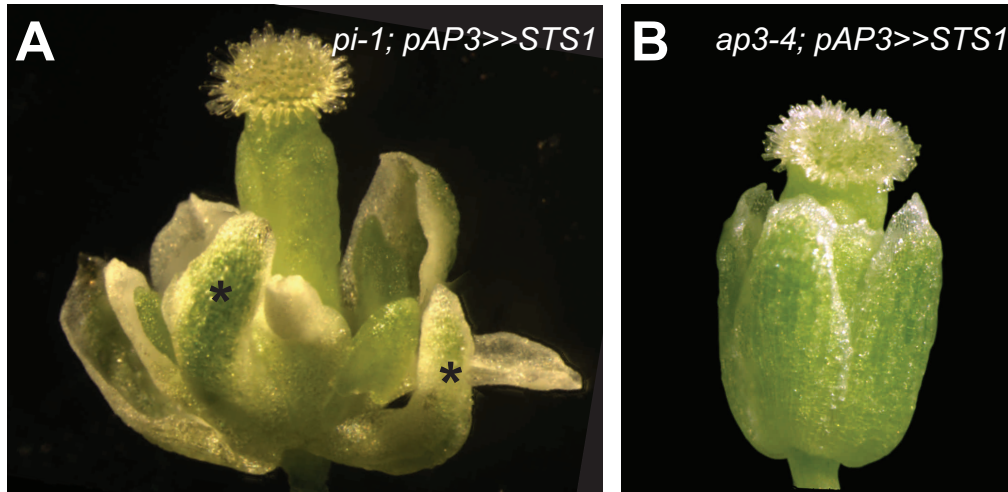


Figure S6. STS1 can rescue the *Arabidopsis* *pi-1* mutant, but not the *ap3-4* mutant. (A) *STS1* under the *AP3* promoter (*pAP3::LhG4>>10-Op::STS1*) showing partial rescue of the *pi-1* mutant phenotype. Sepals have petaloid margins (closest 2 sepals marked with *). (B) The same *STS1* construct under the *AP3* promoter (*pAP3::LhG4>>10-Op::STS1*) does not rescue the *ap3-4* mutant phenotype.

SUPPLEMENTARY REFERENCES

- Bartlett ME, Williams SK, Taylor Z, DeBlasio S, Goldshmidt A, Hall DH, Schmidt RJ, Jackson DP, Whipple CJ 2015. The Maize PI/GLO Ortholog Zmm16/sterile tassel silky ear1 Interacts with the Zygomorphy and Sex Determination Pathways in Flower Development. *The Plant Cell*. doi: 10.1105/tpc.15.00679
- Bouchenak-Khelladi Y, Muasya AM, Linder HP 2014. A revised evolutionary history of Poales: origins and diversification. *Botanical Journal of the Linnean Society* 175: 4-16. doi: 10.1111/boj.12160
- Givnish TJ, Ames M, McNeal JR, McKain MR, Steele PR, dePamphilis CW, Graham SW, Pires JC, Stevenson DW, Zomlefer WB 2010. Assembling the tree of the monocotyledons: plastome sequence phylogeny and evolution of Poales 1. *Annals of the Missouri Botanical Garden* 97: 584-616.
- GPWG II 2012. New grass phylogeny resolves deep evolutionary relationships and discovers C4 origins. *New Phytologist* 193: 304-312. doi: 10.1111/j.1469-8137.2011.03972.x
- Whipple CJ, Ciceri P, Padilla CM, Ambrose BA, Bandong SL, Schmidt RJ 2004. Conservation of B-class floral homeotic gene function between maize and *Arabidopsis*. *Development* 131: 6083-6091.
- Whipple CJ, Schmidt RJ. 2006. Genetics of Grass Flower Development. In: Soltis DE, Leebens-Mack JH, Soltis PS, Callow JA, editors. *Advances in Botanical Research*: Academic Press. p. 385-424.